Effect of Ligand and *n*-Butyl Acrylate on Cobalt-Mediated Radical Polymerization of Vinyl Acetate

Hiromu Kaneyoshi and Krzysztof Matyjaszewski*

Center for Macromolecular Engineering, Department of Chemistry, Carnegie Mellon University, 4400 Fifth Avenue, Pittsburgh, Pennsylvania 15213

Received July 2, 2005; Revised Manuscript Received July 29, 2005

ABSTRACT: The electron-withdrawing effect of the ligand in the cobalt complex was studied in cobalt-mediated radical polymerization of vinyl acetate (VOAc) initiated by 2,2′-azobis(4-methoxy-2,4-dimethylvaleronitrile) (V-70). The polymerization of VOAc with V-70 and a series of bis(acetylacetonate)cobalt derivatives, $Co(R^1COCH{=}COR^2)_2$ ($R^1 = R^2 = CH_3$ (**1**), $R^1 = CF_3$, $R^2 = CH_3$ (**2**), $R^1 = R^2 = CF_3$ (**3**)), was conducted under the same conditions. Complexes **1** and **2** successfully mediated the radical polymerization of VOAc, resulting in poly(VOAc) with predetermined M_n and low polydispersity. In contrast, complex **3** did not control the radical polymerization of VOAc, resulting in poly(VOAc) with higher molecular weight and higher polydispersity. While complex **1** was not able to control the radical polymerization of *n*-butyl acrylate (*n*BA), the copolymerization of *n*BA with various amounts of VOAc (9%, 23%, and 50%) in the presence of V-70 and **1** showed that M_n and M_w/M_n of copolymers decreased with increasing VOAc ratio. This indicated that the extent of control in the copolymerization improved with increasing molar ratio of VOAc. The VOAc content of poly(*n*BA-*co*-VOAc) copolymers was determined by ^{1}H NMR spectroscopy when 50% VOAc was initially added to the copolymerization system. The VOAc content increased with conversion, indicating a gradient sequence distribution in the copolymer. Furthermore, the block copolymer composed of a poly(*n*BA-*grad*-VOAc) segment and a poly(VOAc) block was successfully synthesized when the copolymerization was performed under the VOAc-rich condition (77%) in the initial feed.

Introduction

Recent progress in controlled/living radical polymerization (CRP)[1,2] processes allows synthesis of various well-defined polymer structures in a controlled fashion. Three different CRP mechanisms have been extensively investigated (Scheme 1).[3] The first mechanism (eq 1) is based on a spontaneous reversible homolytic cleavage of a dormant chain end and is exemplified by nitroxide-mediated polymerization (NMP)[4] or cobalt-mediated radical polymerization (CMRP).[5−10] The second process (eq 2) involves a catalytic reversible homolytic cleavage of a carbon−halogen bond via a redox process, which occurs in atom transfer radical polymerization (ATRP).[11−15] The third (eq 3) is based on a thermodynamically neutral bimolecular exchange between growing radicals and a dormant species. Degenerative transfer (DT) polymerization with alkyl iodides[16,17] and reversible addition−fragmentation chain transfer (RAFT)[18] belong in this category.

The mechanism for NMP and CMRP is based on controlling the radical concentration ($P_n^\bullet$) by creation of a dynamic equilibrium between a dormant species (P_n−X) and a stable persistent radical (X$^\bullet$) (eq 1 in Scheme 1). In general, stable persistent radicals include stable organic radicals (e.g., nitroxide[4]) or metal-centered radicals (e.g., cobalt porphyrins[5−7] and bis(acetylacetonate)cobalt complex[8,9]). The general scheme for CMRP is displayed in Scheme 2. After the decomposition of a radical initiator, the created organic radical can react with monomer to form the monomer radical (initiation step). This radical starts polymerization with monomer (propagation step). Meanwhile, the cobalt complex can react with the propagating radical to form a dormant species (deactivation step). A spontaneous homolytic cleavage of a dormant chain end reproduces a propagating chain end radical and a cobalt complex (activation step). The radical concentration in the polymerization system becomes appreciably lower when k_{deact} is much larger than k_{act}, and the equilibrium shifts toward a dormant species. Thus, high ratio of k_{deact}/k_{act} reduces the contribution of chain-breaking reactions compared to a conventional polymerization processes. In addition, the correlation between k_p and k_{deact} is also important to attain a low polydispersity index in the formed polymer (eq 1).[12] According to this equation, polydispersity increases with concentration of dormant species ($[P_n{-}Co^{III}L_n]_0$) and decreases with the concentration of deactivator ($[Co^{II}L_n]$) and with the monomer conversion (p). Furthermore, a lower k_p/k_{deact} value leads to a lower polydispersity index in the polymer. Therefore, a successful CMRP requires simultaneously a high k_{deact}/k_{act} ratio and a relatively low k_p/k_{deact} ratio. As a consequence, the polymer chain is produced in a uniform fashion as in a living polymerization process. Moreover, cobalt complexes may participate in catalytic chain

Scheme 1. Three General Mechanisms for Controlled/Living Radical Polymerization

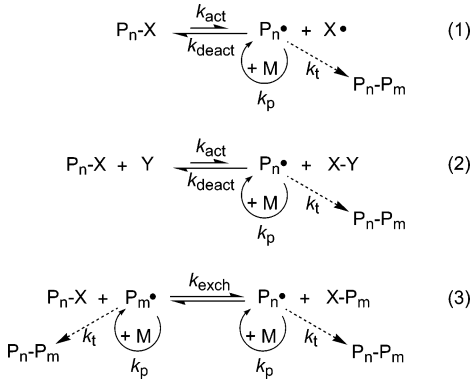

* Corresponding author. E-mail: km3b@andrew.cmu.edu.

10.1021/ma051433v CCC: $30.25
Published on Web 09/02/2005

Scheme 2. General Scheme for Cobalt-Mediated Controlled Radical Polymerization (CMRP)

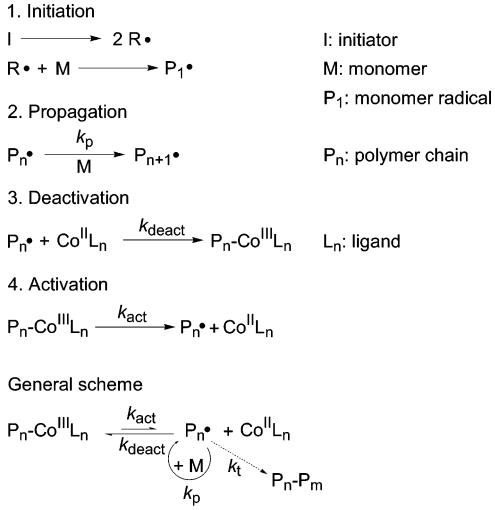

Scheme 3. Molecular Structure of the Cobalt Catalysts Cited in This Study

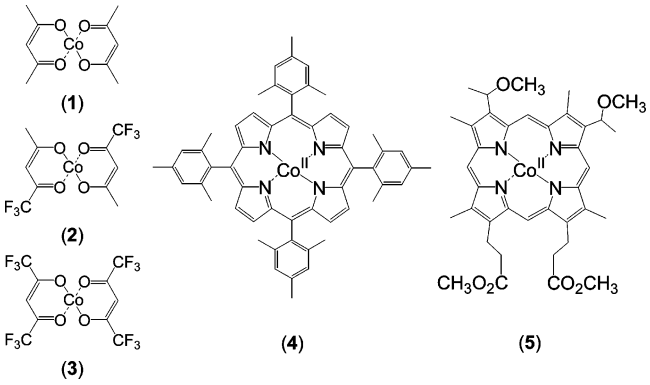

transfer, especially with (meth)acrylates.[19] Such a transfer should be minimized in living system.

$$M_w/M_n = 1 + (k_p[P_n\text{–}Co^{III}L_n]_0/k_{deact}[Co^{II}L_n])(2/p - 1) \quad (1)$$

A spontaneous reversible homolytic cleavage of a dormant chain end is the crucial step for a successful CMRP. As reported in previous papers, the cobalt–porphyrin complex, **4**, can initiate and control a CMRP of acrylates,[5–7] whereas another cobalt–porphyrin complex, **5**, inhibits the polymerization of acrylates[20] despite the similar structure of the ligands (Scheme 3). This difference implies that complex **4** can form a dormant chain end which can be homolytically cleaved after the formation of a dormant species. On the other hand, the cobalt–acrylate bond will be stable in the case of complex **5**. The main differences between these two complexes are the substituents on the porphyrin ligand. Accordingly, changing the steric effect as well as the electron-donating or -withdrawing effect of the substituent on porphyrin ligand affects the extent of dissociation of a dormant chain end.

Recently, a successful CMRP of vinyl acetate (VOAc) was reported.[8] The CMRP was initiated with 2,2′-azobis(4-methoxy-2,4-dimethylvaleronitrile) (V-70) in the presence of bis(acetylacetonate)cobalt(II), complex **1** (Scheme 3). According to this report, complex **1** controlled the polymerization of VOAc. However, **1** was unable to control the radical polymerization of *n*-butyl acrylate (*n*BA) and poly(*n*BA), with relatively high polydispersity indices (2.0–2.2) were obtained. This relatively high polydispersity suggests that the value of k_p/k_{deact} for the polymerization of *n*BA is much higher than that for the polymerization of VOAc. In contrast, the cobalt–porphyrin complex **5** inhibits the polymerization of VOAc[20] despite fact that the complexes have a similar square-planar conformation. This difference in performance between **1** and **5** implies that the ligand influences the electronic state of the cobalt-centered radical. Accordingly, variation of the electronic effect of the ligand may contribute to changes in the value of k_p/k_{deact} and improve the control over the polymerization. In this paper, we report on the effect of electron-withdrawing groups on **1** by comparing the catalytic performance of complexes **1**–**3** in a CMRP of VOAc initiated with V-70 (Scheme 3). Furthermore, we discuss the role of the reaction of a VOAc radical with **1** in the copolymerization of *n*BA with various amounts of VOAc in the presence of V-70.

Experimental Section

Characterization. ^{1}H NMR spectra of the copolymer were examined in deuterated chloroform at 30 °C using a Bruker 300 MHz spectrometer with a delay time 2 s. Conversion of *n*-butyl acrylate (*n*BA) and vinyl acetate (VOAc) monomer was determined by gas chromatography (GC) using a Shimadzu GC 14-A gas chromatograph equipped with a FID detector and ValcoBond 30 m VB WAX Megabore column. *p*-Dimethoxybenzene was used as an internal standard for GC. Molecular weight and molecular weight distribution of the poly(VOAc) and copolymer were measured by gel permeation chromatography (GPC) with PSS columns (styrogel 10^5, 10^3, 10^2 Å) and RI detector. GPC was performed using THF as eluent at a flow rate of 1 mL/min. Molar mass of the poly(VOAc) was determined relative to linear poly(methyl methacrylate) calibration standards. Linear polystyrene calibration standards were used to determine molar mass of the copolymer.

Materials. Nitrogen was purified by passing through the anhydrous calcium sulfate. Vinyl acetate (Aldrich, >99%) and *n*-butyl acrylate (Acros, >99%) were passed through a neutral alumina column to remove stabilizer, dried over calcium hydride, distilled under reduced pressure, and degassed with nitrogen. Toluene (Fisher Scientific, >99%) was distilled over sodium/benzophenone and degassed with nitrogen. Bis(acetylacetonate)cobalt(II) ($Co(acac)_2$; Acros, 99%), bis(trifluoro-2,4-pentanedionato)cobalt(II) ($Co(F3\text{-}acac)_2$; TCI), bis(hexafluoro-2,4-pentanedionato)cobalt(II) ($Co(F6\text{-}acac)_2$; Alfa Aesar, 97%), 2,2′-azobis(4-methoxy-2,4-dimethylvaleronitrile) (V-70; Wako, 96%), and *p*-dimethoxybenzene (Aldrich, 99%) were used as received.

Polymerization of VOAc in the Presence of Cobalt Complexes with V-70. Generally, CMRP was performed as follows, using standard Schlenk techniques. Solvent and monomers were degassed by bubbling with nitrogen for 30 min prior to use. *p*-Dimethoxybenzene (100 mg), $Co(acac)_2$ (28.0 mg, 1.09×10^{-4} mol), and V-70 (33.4 mg, 1.09×10^{-4} mol) were placed in a 25 mL Schlenk flask equipped with a magnetic stirring bar at room temperature. The flask was evacuated by a vacuum pump and backfilled with nitrogen under cooling in a liquid nitrogen bath. This process was repeated three times with cooling. Vinyl acetate (5.0 mL, 5.43×10^{-2} mol) was added to this flask, and the resulting mixture was stirred at room temperature. After taking an initial sample, the reaction was started by heating the mixture to 30 °C. Samples were taken via a syringe periodically to follow the kinetics of the polymerization process. The samples were diluted with toluene followed by filtration through a neutral alumina column and a Gelman Acrodisc 0.2 μm PTFE filter prior to analysis by gas chromatography (GC). After GC measurement, the solvent for the samples was changed to THF for gel permeation chromatography (GPC).

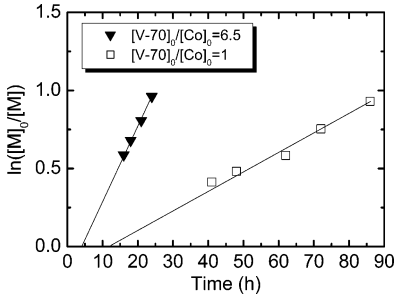

Figure 1. Semilogarithmic kinetic plots for bulk polymerization of VOAc by Co(acac)$_2$ (**1**) with V-70 at 30 °C: (▼) [VOAc]$_0$/[Co]$_0$/[V-70]$_0$ = 500/1/6.5; (□) [VOAc]$_0$/[Co]$_0$/[V-70]$_0$ = 500/1/1.

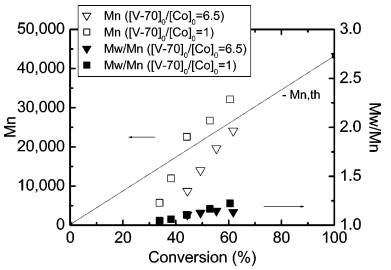

Figure 2. Evolution of M_n and M_w/M_n as a function of VOAc conversion for bulk polymerization of VOAc by Co(acac)$_2$ (**1**) with V-70 at 30 °C: (triangles) [VOAc]$_0$/[Co]$_0$/[V-70]$_0$ = 500/1/6.5; (squares) [VOAc]$_0$/[Co]$_0$/[V-70]$_0$ = 500/1/1.

Copolymerization of *n*BA and VOAc by Co(acac)$_2$ with V-70. The general procedure was similar to that described in detail above. In the case of the initial copolymerization with 23% VOAc in the reaction feed, *p*-dimethoxybenzene (50 mg), Co(acac)$_2$ (19.9 mg, 7.74 × 10^{-5} mol), and V-70 (24.0 mg, 7.74 × 10^{-5} mol) were placed in a 25 mL Schlenk flask. Then vinyl acetate (0.64 mL, 6.94 × 10^{-3} mol) and *n*-butyl acrylate (3.4 mL, 2.32 × 10^{-2} mol) were added to the flask which was then degassed by the vacuum/nitrogen exchange process.

Results and Discussion

Effect of the Electron-Withdrawing Group in 1 on CMRP of VOAc Initiated with V-70. According to a recent paper,[8] CMRP of VOAc with complex **1** proceeded in controlled manner despite used excess radical initiator ([V-70]$_0$/[**1**]$_0$ = 6.5). One polymer chain was formed per one cobalt complex. This suggested low initiation efficiency of V-70 and efficient formation of a dormant species, preventing the uncontrolled free radical polymerization of VOAc. However, 1 equiv of V-70 to cobalt complex should be enough to accomplish CMRP, if one cobalt complex can mediate growth of only one polymer chain. Therefore, initially the effect of varying the ratio of V-70 to cobalt complex was examined. When excess radical initiator was used ([V-70]$_0$/[**1**]$_0$ = 6.5), the induction period became shorter, and the rate of monomer consumption was relatively faster than the reaction when 1 equiv of V-70 to cobalt (Figure 1) was employed. The shorter induction period suggests that excess radical initiator accelerates the formation of dormant species. Furthermore, while the M_n of poly(VOAc) increased with conversion in both cases (Figure 2), the evolution of M_n did not follow a theoretical line calculated based on the living polymerization process in both cases. Indeed, M_n of poly(VOAc) was always lower than the theoretical M_n when excess radical initiator was used. This result demonstrates that more polymer chains were generated from the initiator. However, the polydispersity index of poly(VOAc) remained below 1.3 in both cases. No polymer peak was detected by GPC at a low monomer conversion although some monomer consumption was observed by GC. The poly(VOAc) with low molecular weight and with cobalt species at a chain could be trapped by an alumina column during purification. The purification process was necessary to avoid any damage of GPC columns. Apparently, the content of cobalt species in higher molecular weight polymers was sufficiently small, and they passed through an alumina column without being trapped.

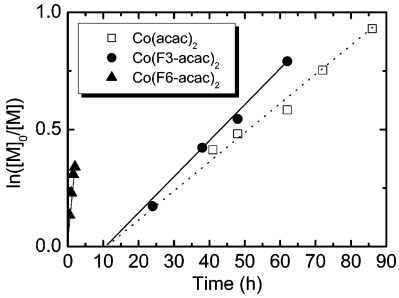

Figure 3. Semilogarithmic kinetic plots for bulk polymerization of VOAc by cobalt complexes with V-70 at 30 °C: [VOAc]$_0$/[Co]$_0$/[V-70]$_0$ = 500/1/1; (□) Co(acac)$_2$ (**1**), (●) Co(F3-acac)$_2$ (**2**), (▲) Co(F6-acac)$_2$ (**3**).

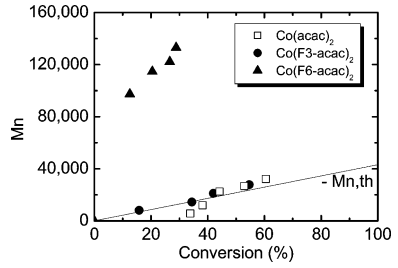

Figure 4. Evolution of M_n vs VOAc conversion for bulk polymerization of VOAc with different cobalt complexes and V-70 at 30 °C: [VOAc]$_0$/[Co]$_0$/[V-70]$_0$ = 500/1/1; (□) Co(acac)$_2$ (**1**), (●) Co(F3-acac)$_2$ (**2**), (▲) Co(F6-acac)$_2$ (**3**).

As mentioned above, the CMRP of VOAc mediated by **1** showed an induction period. This suggested that formation of the dormant species at the initial step is the dominant reaction due to the sufficiently large k_{deact} under this condition. Therefore, we assumed that changing the electronic effect of the ligand may affect the k_{deact} and also k_{act} values in the polymerization because of a change of the reactivity of cobalt complex. Accordingly, CMRPs of VOAc were conducted in the presence of cobalt complexes with ligands containing electron-withdrawing groups and V-70 to confirm this hypothesis. We selected bis(trifluoro-2,4-pentanedionato)cobalt(II) (Co(F3-acac)$_2$, **2**) and bis(hexafluoro-2,4-pentanedionato)cobalt(II) (Co(F6-acac)$_2$, **3**) to systematically investigate the effect of electron-withdrawing groups (Scheme 3). The initial molar ratio of V-70 to cobalt complex was set at 1. As expected, fairly different results were obtained with complexes **1**−**3**. The semilogarithmic kinetic plots showed three different slopes (Figure 3). Long induction periods (>10 h) were observed in the case of **2** as well as **1**. In contrast, no induction period was observed for **3**, and the VOAc monomer was consumed much faster than with **2**. As shown in Figure 4, the M_n of poly(VOAc) increased along a theoretical line calculated on the basis of the assumption of living polymerization process in the case of **2**. On the other hand, a large departure from the theoretical M_n was observed for the poly(VOAc) formed in the

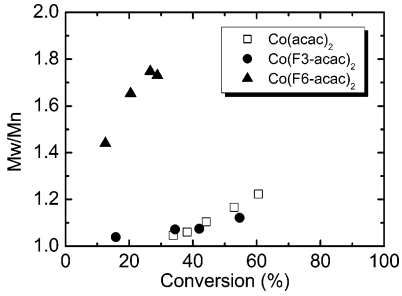

Figure 5. Evolution of M_w/M_n vs VOAc conversion for bulk polymerization of VOAc by cobalt complexes and V-70 at 30 °C: $[VOAc]_0/[Co]_0/[V\text{-}70]_0 = 500/1/1$; (□) $Co(acac)_2$ (**1**), (●) $Co(F3\text{-}acac)_2$ (**2**), (▲) $Co(F6\text{-}acac)_2$ (**3**).

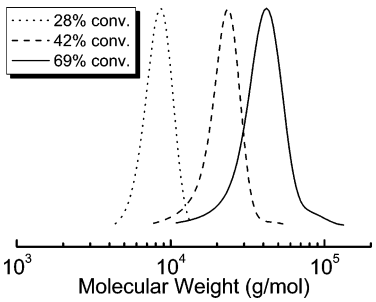

Figure 6. GPC traces of poly(VOAc) prepared with $Co(F3\text{-}acac)_2$ (**2**) and V-70 at 30 °C: $[VOAc]_0/[\mathbf{2}]_0/[V\text{-}70]_0 = 500/1/1$.

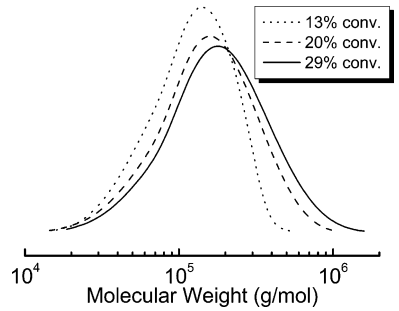

Figure 7. GPC traces for poly(VOAc) prepared with $Co(F6\text{-}acac)_2$ (**3**) and V-70 at 30 °C: $[VOAc]_0/[\mathbf{3}]_0/[V\text{-}70]_0 = 500/1/1$.

presence of **3**, indicating that the reaction of the VOAc radicals with **3** is much slower than with **1** and **2**. Furthermore, the M_w/M_n of poly(VOAc) formed in the presence of **2** remained below 1.2 (Figure 5). GPC traces showed clear peak shift toward high molecular weight region with monomodal shape, as was the case with **1**[8] (Figure 6). These observations supported the absence of uncontrolled free radical polymerization. Whereas in the case of **3**, the M_w/M_n increased with conversion, up to 1.7, and GPC traces exhibited broad monomodal peaks (Figure 7), indicating inefficient deactivation. This was also supported by the remaining orange color, typical for Co(II) species of **3**. In contrast, with **2**, polymerization started only after color was changed from orange (Co(II)) to brown (Co(III)).

Copolymerization of *n*BA with Various Amounts of VOAc by 1 in the Presence of V-70. According to a recent report,[8] complex **1** cannot control the radical polymerization of *n*BA in the presence of V-70. In addition, conversion of *n*BA was unreliably low (5% after 3 h). We conducted polymerization of *n*BA under a similar condition, $([n\text{BA}]_0/[\mathbf{1}]_0/[V\text{-}70]_0 = 500/1/1$ at 30 °C). The reaction mixture rapidly turned viscous, and a gel was formed after 25 min. The semilogarithmic kinetic plot for the polymerization of *n*BA displayed a

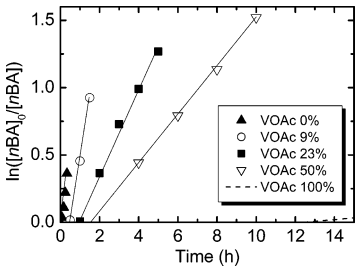

Figure 8. Semilogarithmic kinetic plots for bulk copolymerization of *n*BA and VOAc with $Co(acac)_2$ (**1**) and V-70 at 30 °C: $([n\text{BA}]_0 + [VOAc]_0)/[Co]_0/[V\text{-}70]_0 = (330-500)/1/1$.

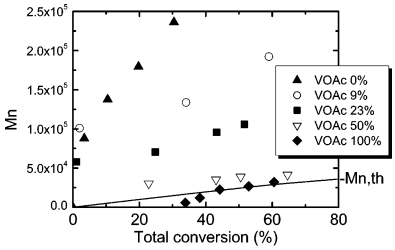

Figure 9. Evolution of M_n vs total monomer conversion for bulk copolymerization of *n*BA and VOAc with $Co(acac)_2$ (**1**) and V-70 at 30 °C: $([n\text{BA}]_0 + [VOAc]_0)/[Co]_0/[V\text{-}70]_0 = (330-500)/1/1$.

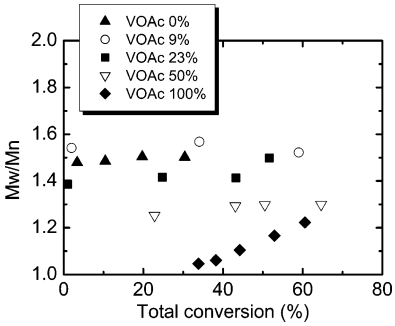

Figure 10. Evolution of M_w/M_n vs total monomer conversion for bulk copolymerization of *n*BA and VOAc with $Co(acac)_2$ (**1**) and V-70 at 30 °C: $([n\text{BA}]_0 + [VOAc]_0)/[Co]_0/[V\text{-}70]_0 = (330-500)/1/1$.

fast rate for *n*BA consumption (VOAc 0% in Figure 8). Furthermore, GPC traces for poly(*n*BA) revealed that the M_n of poly(*n*BA) increased monotonously with conversion (VOAc 0% in Figure 9), and the M_w/M_n of poly(*n*BA) remained about 1.5 (VOAc 0% in Figure 10). These data indicated that complex **1** has the potential to mediate a CMRP of *n*BA, although the k_p/k_{deact} ratio is much higher than for VOAc. The significantly lower value of k_p/k_{deact} for VOAc could be exploited to control the polymerization of *n*BA in the presence of VOAc. Therefore, *n*BA was copolymerized with various amounts of VOAc (9, 23, and 50 mol %) using **1** and V-70 ($[V\text{-}70]_0/[\mathbf{1}]_0 = 1$) at 30 °C in order to examine the contribution of VOAc to the process and determine whether one could extend control to the copolymerization.

As shown in Figure 8, the semilogarithmic kinetic plots for the *n*BA copolymerizations were linear in each case. As anticipated, an induction period emerged after the addition of VOAc, suggesting that the selective coupling between the VOAc-terminated polymer radical (or initiator fragment) and **1** proceeded successfully in the copolymerization system. Moreover, the induction period was longer, and the slope of lines decreased with increasing proportion of VOAc in the copolymerization. This suggested that increase of the molar ratio of VOAc

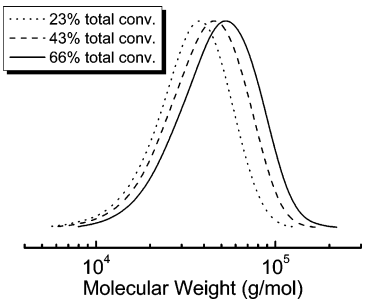

Figure 11. GPC traces for poly(*n*BA-*co*-VOAc) prepared with $Co(acac)_2$ (**1**) and V-70 at 30 °C: $[nBA]_0/[VOAc]_0/[Co]_0/[V\text{-}70]_0 = 200/200/1/1$ (VOAc 50%).

strongly shifted the equilibrium toward the dormant species. The evolutions of M_n and M_w/M_n for the copolymers as a function of total conversion were exhibited in Figures 9 and 10, respectively. The M_n of the copolymers increased monotonously with total conversion, indicating somehow controlled copolymerization (Figure 9). The slope of lines decreased with increasing VOAc ratio, suggesting smaller values for k_p/k_{deact} with increasing proportion of VOAc. At the same total conversion, the M_n of copolymer decreased with increasing VOAc ratio. This demonstrated that the number of initiated polymer chains increased with increasing VOAc ratio, presumably due to the higher coupling efficiency of the chain end VOAc radical to cobalt during the copolymerization. Furthermore, the M_w/M_n of the copolymer also decreased with increasing proportion of VOAc (Figure 10). These data indicated that the degree of control over copolymerization improved with increasing molar ratio of VOAc. A lower polydispersity index for the polymer can be correlated with a lower k_p/k_{deact} ratio (eq 1). As shown in Figure 11, GPC traces for resulting poly(*n*BA-*co*-VOAc) exhibit monomodal peaks in all cases.

The composition of the poly(*n*BA-*co*-VOAc) copolymer, obtained when 50% VOAc was initially added to the copolymerization system, was investigated by ^{1}H NMR to examine the incorporation and distribution of VOAc of the copolymer. The representative spectrum is shown in Figure 12. Peaks originating from *n*BA and VOAc segments were observed in the spectrum, indicating successful copolymerization. The VOAc content was evaluated from the integrals of signals labeled a−c in Figure 12, and the results are plotted in Figure 13. According to the previous report, the monomer reactivity ratios of *n*BA and VOAc determined using the integrated Meyer−Lowry or Finneman−Ross equations were $r_{nBA} = 10.7$ or 12 and $r_{VOAc} = 0.02$, respectively.[21] It was not possible to accurately determine the consistent reactivity ratios from NMR experiments using the joint confidence intervals (JCI) or Kelen−Tüdõs equations. However, the experimental NMR data provided the best fit with slightly higher $r_{nBA} \sim 15$. The instantaneous and cumulative VOAc contents in the copolymer based on $r_{nBA} = 15$ and $r_{VOAc} = 0.02$ are plotted together with the NMR results in Figure 13. The VOAc content in copolymer, estimated by ^{1}H NMR, increased with total conversion, indicating a gradient sequence distribution in the copolymer. According to a curve of instantaneous VOAc content, a block copolymer composed of a poly(*n*BA-*grad*-VOAc) segment and a poly(VOAc) segment should be obtained when the bulk copolymerization is extended to over 64% total conversion.

Synthesis of Poly(*n*BA-*grad*-VOAc)-*block*-poly(VOAc) by CMRP. The copolymerization of *n*BA and VOAc was conducted at VOAc 77% in the initial feed to synthesize a block copolymer composed of a poly(*n*BA-*grad*-VOAc) segment and a pure poly(VOAc) segment. Toluene (30 vol %) was used as a solvent to decrease the viscosity of the reaction medium. The monomer conversion measured by GC indicated that the *n*BA monomer was completely consumed within 21 h, and subsequently the consumption of VOAc was observed until 95 h (Figure 14). The half-life of V-70 in toluene was 10 h at 30 °C, and therefore, the majority of initiator should have decomposed to create the initiator radical after 20 h. Thus, the monomer consumption of VOAc after 20 h should result in the formation of a block copolymer. In addition, the M_n of the resulting copolymer increased with total conversion as polydispersity maintained below 1.3 (Figure 15). The departure from

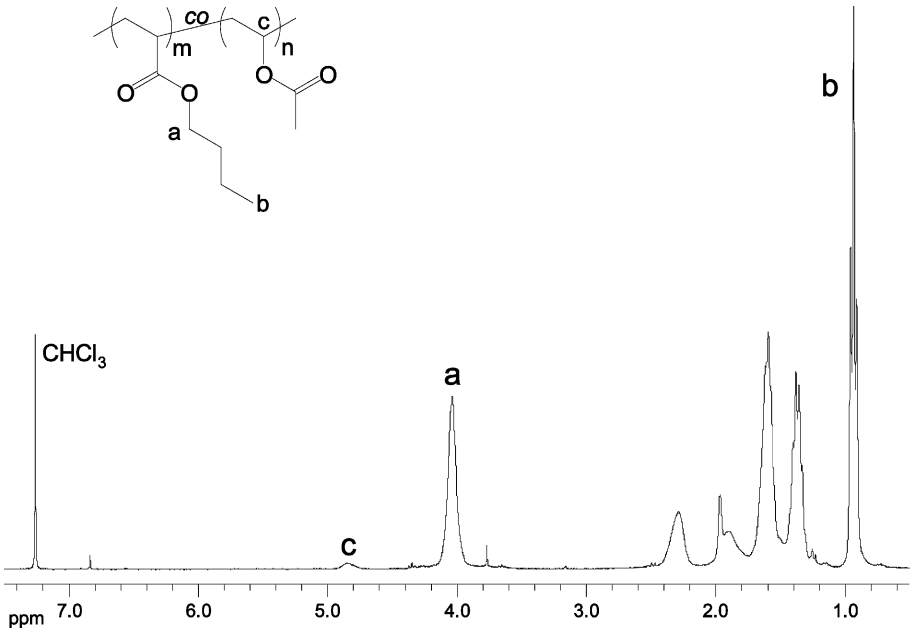

Figure 12. ^{1}H NMR spectrum of poly(*n*BA-*co*-VOAc) in $CDCl_3$ at 30 °C (300 MHz): $[nBA]_0/[VOAc]_0/[Co]_0/[V\text{-}70]_0 = 200/200/1/1$ at 30 °C (total conversion 51%).

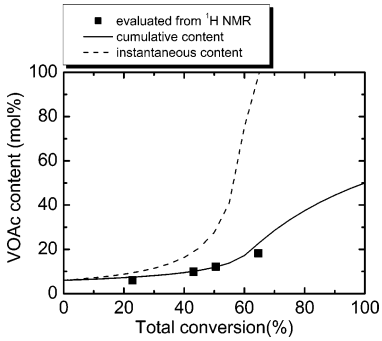

Figure 13. VOAc content in a poly(*n*BA-*co*-VOAc) copolymer as a function of total conversion: $[n\text{BA}]_0/[\text{VOAc}]_0/[\text{Co}]_0/[\text{V-70}]_0 = 200/200/1/1$ at 30 °C. Lines calculated using $r_{\text{nBA}} = 15$ and $r_{\text{VOAc}} = 0.02$.

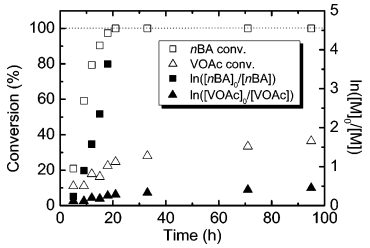

Figure 14. Dependence of monomer conversion on time and semilogarithmic kinetic plots for copolymerization of *n*BA and VOAc with Co(acac)$_2$ (**1**) and V-70 at 30 °C: $[n\text{BA}]_0/[\text{VOAc}]_0/[\text{Co}]_0/[\text{V-70}]_0 = 90/300/1/1$, monomer/toluene = 70/30 (v/v).

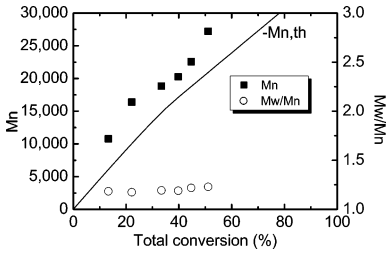

Figure 15. Evolution of M_n and M_w/M_n as a function of total monomer conversion for copolymerization of *n*BA and VOAc with Co(acac)$_2$ (**1**) and V-70 at 30 °C: $[n\text{BA}]_0/[\text{VOAc}]_0/[\text{Co}]_0/[\text{V-70}]_0 = 90/300/1/1$, monomer/toluene = 70/30 (v/v).

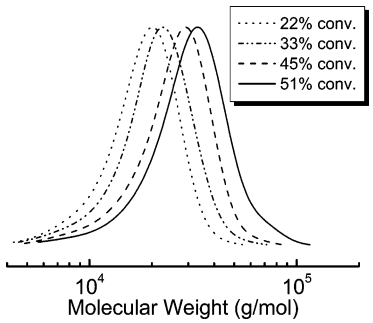

Figure 16. GPC traces for poly(*n*BA-*grad*-VOAc)-*block*-poly(VOAc) prepared with Co(acac)$_2$ (**1**) and V-70 at 30 °C: $[n\text{BA}]_0/[\text{VOAc}]_0/[\text{Co}]_0/[\text{V-70}]_0 = 90/300/1/1$, monomer/toluene = 70/30 (v/v).

theoretical line calculated on the basis of the living polymerization process was observed, as was the case of other copolymerizations. Moreover, GPC traces for copolymers exhibited monomodal shapes, and these significantly shifted toward the high molecular weight region (Figure 16). No peak appeared at the low molecular weight region, supporting the absence of homopoly(VOAc). This demonstrated that the chain growth

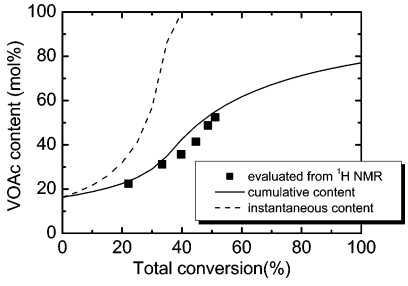

Figure 17. VOAc content in a growing poly(*n*BA-*grad*-VOAc)-*block*-poly(VOAc) as a function of total conversion: $[n\text{BA}]_0/[\text{VOAc}]_0/[\text{Co}]_0/[\text{V-70}]_0 = 90/300/1/1$ at 30 °C, monomer/toluene = 70/30 (v/v). Lines calculated using $r_{\text{nBA}} = 15$ and $r_{\text{VOAc}} = 0.02$.

of poly(VOAc) proceeded successfully from the chain end of poly(*n*BA-*grad*-VOAc) without losing control over polymerization.

The instantaneous and cumulative VOAc content of the copolymer based on the reactivity ratios $r_{\text{nBA}} = 15$ and $r_{\text{VOAc}} = 0.02$ and the experimental results from ^{1}H NMR are shown in Figure 17. The variation of instantaneous VOAc content suggested that all of *n*BA monomer should be consumed at 40% total conversion. Therefore, from 40 to 51% total conversion only VOAc was consumed, leading to the pure poly(VOAc) segment. This leads to a block copolymer containing a poly(*n*BA-*grad*-VOAc) segment and a pure poly(VOAc) segment.

Conclusion

In a CMRP of VOAc the k_p/k_{deact} ratio for the polymerization drastically changed when the electron-withdrawing effect of the ligand was increased. This was presumably due to the change of the value of k_{deact} caused by a change in the reactivity of the cobalt species toward the VOAc radical. Therefore, modifying the electronic effects of the ligand should allow a desired ratio of k_p/k_{deact} to be attained. The Co(acac)$_2$ complex **1** could provide controlled copolymerization of *n*BA in the presence of VOAc. As anticipated, a lower ratio of k_p/k_{deact} for VOAc polymerization strongly allowed control of the CMRP of *n*BA, particularly when the mole fraction of VOAc in the copolymerization was high. The effect of the amount of VOAc added to the reaction on M_n, M_w/M_n, and monomer sequence distribution of copolymer indicated that deactivation of the chain end VOAc radical by **1** was the critical step to control this copolymerization.

Acknowledgment. We greatly appreciate the financial support from the National Science Foundation (DMR-0090409 and CHE-0405627) and Mitsui Chemicals, Inc.

References and Notes

(1) Matyjaszewski, K., Ed.; *Advances in Controlled/Living Radical Polymerization;* ACS Symposium Series Vol. 854; American Chemical Society: Washington, DC, 2003.
(2) Matyjaszewski, K., Davis, T. P., Eds.; *Handbook of Radical Polymerization*; Wiley-Interscience: Hoboken, NJ, 2002.
(3) Goto, A.; Fukuda, T. *Prog. Polym. Sci.* **2004**, *29*, 329.
(4) Hawker, C. J.; Bosman, A. W.; Harth, E. *Chem. Rev.* **2001**, *101*, 3661.
(5) Wayland, B. B.; Poszmik, G.; Mukerjee, S. L.; Fryd, M. *J. Am. Chem. Soc.* **1994**, *116*, 7943.
(6) Wayland, B. B.; Basickes, L.; Mukerjee, S.; Wei, M.; Fryd, M. *Macromolecules* **1997**, *30*, 8109.
(7) Lu, Z.; Fryd, M.; Wayland, B. B. *Macromolecules* **2004**, *37*, 2686.

(8) Debuigne, A.; Caille, J.-R.; Jerome, R. *Angew. Chem., Int. Ed.* **2005**, *44*, 1101.
(9) Debuigne, A.; Caille, J.-R.; Detrembleur, C.; Jerome, R. *Angew. Chem., Int. Ed.* **2005**, *44*, 3439.
(10) Arvanitopoulos, L. D.; Greuel, M. P.; King, B. M.; Shim, A. K.; Harwood, H. J. In *Controlled Radical* Polymerization; ACS Symposium Series Vol. 685; Matyjaszewski, K., Ed.; American Chemical Society: Washington, DC, 1998; p 316.
(11) Kamigaito, M.; Ando, T.; Sawamoto, M. *Chem. Rev.* **2001**, *101*, 3689.
(12) Matyjaszewski, K.; Xia, J. *Chem. Rev.* **2001**, *101*, 2921.
(13) Patten, T. E.; Xia, J.; Abernathy, T.; Matyjaszewski, K. *Science* **1996**, *272*, 866.
(14) Wang, J.-S.; Matyjaszewski, K. *J. Am. Chem. Soc.* **1995**, *117*, 5614.
(15) Wang, J.-S.; Matyjaszewski, K. *Macromolecules* **1995**, *28*, 7901.
(16) Gaynor, S. G.; Wang, J.-S.; Matyjaszewski, K. *Macromolecules* **1995**, *28*, 8051.
(17) Iovu, M. C.; Matyjaszewski, K. *Macromolecules* **2003**, *36*, 9346.
(18) Chiefari, J.; Rizzardo, E. In *Handbook of Radical Polymerization*; Matyjaszewski, K., Davis, T. P., Eds.; Wiley-Interscience: Hoboken, NJ, 2002; p 629.
(19) Gridnev, A. A.; Ittel, S. D. *Chem. Rev.* **2001**, *101*, 3611.
(20) Enikolopyan, N. S.; Smirnov, B. R.; Ponomarev, G. V.; Belgovskii, I. M. *J. Polym. Sci., Part A: Polym. Chem.* **1981**, *19*, 879.
(21) Bataille, P.; Bourassa, H. *J. Polym. Sci., Part A: Polym. Chem.* **1989**, *27*, 357.

MA051433V